



Strategies to engineer FeCoNiCuZn high entropy alloy composition through aqueous electrochemical deposition

Kunda Siri Kiran Janardhana Reddy, L.P. Pavithra Chokkakula^{*}, Suhash Ranjan Dey^{*}

Combinatorial Materials Lab, Department of Materials Science and Metallurgical Engineering, Indian Institute of Technology Hyderabad, Kandi, Sangareddy 502284, India

ARTICLE INFO

Keywords:

High entropy alloy
Aqueous electrodeposition
Thin film
Duty cycle

ABSTRACT

Low melting point elements are often incompatible with alloy synthesis methods that involve high temperatures, and thus, high entropy alloys containing zinc (Zn) have not been explored much to date, hindering the development of new alloy system investigations. In such cases, electrodeposition can be a useful alternative for the synthesis of multi-component (MCA)/high entropy alloys (HEA) which contain elements with large differences in their melting point and those that cannot be easily synthesized through established conventional/melting-casting routes. Though electrodeposition is an age-old technique, exploration of this synthesis route for fabricating HEAs is recently gaining attention, and more specifically, aqueous medium electrodeposition is still in its infancy. The current work reports a HEA containing Zn, namely, FeCoNiCuZn, through electrodeposition in an aqueous medium utilizing sulfate salts. Electrodeposition was carried out by varying different input parameters, namely, duty cycles (input pulse parameters), pH, and substrate roughness. Through these different input parameters, their effects on the composition, phase, and morphology of the deposited films are a matter of investigation. Observations revealed that the composition of the electrodeposited FeCoNiCuZn thin film is highly dependent on the input pulse parameters and the pH, whereas the substrate roughness played no observable significant role, probably owing to the use of pulsed waveform and the very low film thickness (~ 500 nm). The compositional characterization of the electrodeposited FeCoNiCuZn showed the presence of a high percentage of Cu (> 50 at.%) at lower duty cycles (< 0.75), whereas higher duty cycle (> 0.75) resulted in FeCoNiCuZn HEAs with all five elements in almost equal proportion. Alternatively, lower pH (≤ 1.5) led to high Cu content in the thin film, whereas higher pH (≥ 2.5) resulted in a multi-elemental deposition.

1. Introduction

Materials selection and design are some critical aspects for structural and functional applications, where the combination and composition of the elements play a major role in deciding the properties of the material. Recently, high entropy alloys (HEAs) having more than 5 elements are receiving attention as possible alternatives to replace conventionally used materials where the high mixing entropy in HEAs is supposedly responsible for stabilizing the system into simple phases [1,2]. Therefore, research on HEAs for possible structural applications has been explored to a great extent. However, functional applications of these alloys, especially in the form of thin films and other nanostructures, have not been fully explored owing to various challenges. Though thin film coating techniques like magnetron sputtering [3] and pulsed laser deposition [4,5] have been reported to synthesize HEAs, their scalability

and viability remain a challenge due to their stringent process requirements. On the other hand, electrodeposition (ED) can also be used for the deposition of thin films and can be undertaken at ambient conditions with a simple experimental setup that can be an alternative approach to address these rigorous process requirements. Additionally, the immense control over the surface morphology, phases, grain size, as well as composition, are some advantages of ED that make it an interesting tool for the deposition of thin films. Further, ED allows coatings of elements irrespective of their miscibility, melting points, etc. which can bypass the conventional rules for making alloys. For instance, HEAs containing Zn remain unexplored as they are difficult to process on account of the low melting point compared to conventionally used metals like iron (Fe), cobalt (Co), nickel (Ni), etc., through melting-casting routes. Unlike the conventional metallurgical approaches, electrodeposition relies on the reduction potentials of the elements and can be a

^{*} Corresponding authors.

E-mail addresses: pavithra.ch@msme.iith.ac.in (L.P.P. Chokkakula), suhash@msme.iith.ac.in (S.R. Dey).

<https://doi.org/10.1016/j.electacta.2023.142350>

Received 12 January 2023; Received in revised form 7 March 2023; Accepted 31 March 2023

Available online 1 April 2023

0013-4686/© 2023 Elsevier Ltd. All rights reserved.

suitable approach for the deposition of HEAs containing elements like Zn.

In this direction, very few reports exist on the use of electrodeposition to fabricate HEA thin films. Initial reports on HEA electrodeposition suggested the use of organic electrolytes where BiFeCoNiMn [6], TmFeCoNiMn [7], MgMnFeCoNiGd [8], and AlCrFeMnNi, AlCrCuFeMnNi alloys [9] were fabricated. Further, few reports also exist on using non-aqueous solvents to deposit HEAs having Zr, Ti where elements with larger reduction potentials and those that cannot be deposited in an aqueous medium have been electrodeposited [10–12]. Although organic and non-aqueous electrolytes have been explored to some extent in synthesizing the HEAs, they are expensive, toxic, and industrial scalability is challenging [13]. The usage of aqueous electrolytes for HEA synthesis has still not materialized much due to the challenges of H₂ evolution. However, electrodeposition through an aqueous medium can become superior over organic and non-aqueous means by proper control over the mechanisms and experimental inputs [14–16]. The aqueous medium for the deposition of alloys is a preferred choice as it drastically reduces the cost involved in depositing alloy thin films and is also environmentally friendly. Therefore, through this study, we attempted to engineer the FeCoNiCuZn HEA thin film containing Zn (low melting point) fabricated using an electrodeposition route in an aqueous medium [17,18]. Engineering the HEA was undertaken by varying the experimental parameters such as duty cycles, pH, and substrate roughness, as these parameters may significantly control the composition and microstructure of the HEAs. The influence of the duty cycle on the various properties of non-aqueous electrodeposited thin films of CoCrFeMnNi was reported earlier, where it was observed that the pulse parameters strongly influenced the composition and as well as the crystallite size of the non-aqueous electrodeposited thin films [19,20]. Unlike the non-aqueous routes, hydrogen evolution reactions that take place in the aqueous route can alter deposition kinetics by changing the pH near the electrode surface, giving rise to drastic changes in composition. On the other hand, the surface roughness dictates the nature of the diffusion zones and also influences the overall composition, homogeneity as well as morphology of the electrodeposited thin films [21]. These parameters play a very important role in deciding the final properties of the electrodeposited alloy and, to the best of our knowledge, such studies on aqueous electrodeposited materials have not yet been undertaken. Therefore, this investigation in an aqueous medium for optimizing the experimental parameters can provide a strategy for designing new HEAs/MCAs, which will help in exploring the compositional space and mapping their respective properties.

2. Materials and methods

2.1. Electrolyte preparation

The current electrolyte (Table S1) consisted mainly of sulphates of Fe, Co, Ni, Cu, and Zn. Sodium citrate and boric acid were used as complexing agent and buffer, respectively [17]. De-ionized water of 18.2 M Ω was used as the medium for electrolyte preparation. H₂SO₄ was utilized during electrolyte preparation to prevent precipitation of the salts, which may occur during electrolyte preparation, and to maintain the pH. After preparing the electrolyte by adding all the salts, the as-prepared electrolyte pH was considered the initial/optimized pH and was further employed for the electrodeposition study. All depositions were carried out in a three-electrode configuration (Autolab PGSTAT 204) with platinum as the counter, Ag/AgCl (3 M NaCl) as the reference electrode, and Ti sheet as a working electrode (area for deposition is considered as 1 cm²).

2.2. Duty cycle study

For the current investigations, depositions of FeCoNiCuZn were

carried out at a potential of -1.5 V with varied duty cycles as direct current (DC) and pulsed voltages (PC) modes. It is well known that PC mode is preferred over DC mode. Unlike a constant supply in DC, in PC, the current/voltage is repeatedly switched ON (T_{on}) and OFF (T_{off}) at regular intervals. It is already a fact that the T_{on} plays a critical role in nucleation and growth dynamics, whereas the T_{off} aids in surface diffusion, corrosion, and desorption [22]. The applied duty cycle ($T_{on} * (T_{on} + T_{off})^{-1}$) was varied by changing the T_{on} and T_{off} times. T_{on} time of 10, 20, 30, 40 & 50 milli sec (ms) and T_{off} times of 10, 20, 30, 40 & 50 ms were employed to investigate the effects of duty cycles on the composition of the electrodeposited thin film. A set of 25 samples were synthesized using these duty cycles, and this was followed by a constant (DC) voltage electrodeposition (as a 100% duty cycle for comparison) which makes a total of 26 samples. As prepared electrolyte pH (~ 2.5) was employed for all the above 26 electrodepositions. To simplify and for better understanding, four samples with duty cycles of 16.67%, 50.00%, 83.33%, and 100% were considered and named as low duty cycle (LD), intermediate duty cycle (ID), high duty cycle (HD) and direct current (DC) sample for further characterization.

2.3. Substrate roughness & pH study

Similarly, the role of substrate roughness and pH of the electrolyte were also investigated simultaneously. To study the role of substrate roughness, initially, different titanium (Ti) substrates were polished on different grades of SiC papers, namely, 80, 600, 1500, and 2500 grit to induce various levels of surface roughness. A final polishing on the vibromet was also undertaken with the help of colloidal silica. These substrate samples were named 80, 600, 1500, 2500, and vibromet, depending on the polishing level. The polished Ti foils with various levels of surface roughness were utilized to study the role of surface roughness by employing the optimized duty cycle where HEA composition was attained. Similarly, the pH of the electrolyte has a significant role in deciding the composition of the HEA, and electrolyte with various pH (pH = 0.5, 1.5, 2.5, 3.5, and 4.5) has been prepared using either concentrated H₂SO₄ or NaOH. It was noticed that pH ≥ 5 of the electrolyte leads to precipitation, and therefore our study was limited to pH ≤ 4.5 .

2.4. Characterization studies

As a preliminary step, cyclic voltammetry (CV) studies were conducted for electrolytes with sodium citrate and boric acid containing single metal ions (five various electrolytes) and an electrolyte containing all five metal ions using glassy carbon as the working electrode (scan rate of 50 mV/s) from 0.75 V to -1.75 V and reversed back to 0.75 V to understand the electrochemical behavior/reduction of the electrolyte containing multiple metal ions. The electrodeposited samples synthesized at various applied experimental parameters were further considered for microstructural and composition analysis. The electrodeposited thin films were analyzed by JEOL field emission scanning electron microscopy (FE-SEM JEOL JIB 4700F) at 20 kV having a working distance of 10 ± 1 mm for their microstructure/morphology analyses, whereas the elemental composition of the thin films was analyzed using energy dispersive spectroscopy (EDS) attached to the FE-SEM. Further, the crystal structure of the selected electrodeposited films was determined using powder XRD (Rigaku Ultima IV) at a scan rate of 0.02° per minute. On the other hand, atomic force microscopy (AFM) studies (Park NX 10 SPM) were also undertaken in contact mode to report the surface roughness of the various Ti substrates before and those of the thin films after depositions.

3. Results and discussion

3.1. Cyclic voltammetry study

CV studies of individual electrolytes with the single metal ion in the presence of a complexing agent and boric acid were initially undertaken (Fig. S1), where reduction peaks at different potentials corresponding to different elements could be seen. However, the cyclic voltammetry studies of the as-prepared electrolyte containing all the 5 metal ions (Fe, Co, Ni, Cu, Zn) showed a completely different picture. As seen in Fig. 1, the current initially starts reducing from 0.75 V as it moves towards more negative values, and it remains constant till -0.10 V. When increasing the polarization further to more negative values, an increase in current is observed which corresponds to the reduction of Cu ions from the electrolyte at approx. -0.18 V. After reaching the peak current at -0.18 V, the current reduces till -0.5 V and is further stable till -1.0 V. From -1.0 V onwards, the cathodic current again increases till -1.46 V, which can be ascribed to the reduction of the Fe, Co, Ni, and Zn ions from the electrolyte. After -1.52 V, H_2 evolution occurs which is marked in blue in Fig. 1. There are two crossover points at ~ -1.25 V and ~ -0.8 V during the reverse positive sweep. The exact physical nature of the crossover is not well defined and ambiguous. However, it is well-accepted that the crossover points in the CV are probably an indication of nucleation [23,24]. From the observations in the CV, as the peak reduction was obtained at -1.46 V for the electrolyte, a potential of -1.5 V was employed to reduce all the multiple metal ions (5 elements) for all the electrodepositions in the current study.

3.2. Duty cycle study (Variation of T_{on} & T_{off})

As mentioned in Section 2.2, duty cycles (i.e. variation of T_{on} & T_{off}) play a major role in controlling the morphology and composition, especially in alloys prepared by electrodeposition. Microstructural and morphological characterization of the prepared samples at various duty cycles were analyzed using FE-SEM, whereas EDS analysis was used for compositional quantification and to analyze compositional changes. The FE-SEM images (Fig. 2) confirm the deposition on the Ti substrate without any morphological differences. Further, the FE-SEM images also reveal the presence of uniform globular-shaped entities, which is very common in electrodeposition. The globular microstructure can also be on account of the diffusion-controlled process, which arises as a result of the depletion of metal ions near the cathode [25], the use of complexing agents [26], and the use of pulse parameters. The

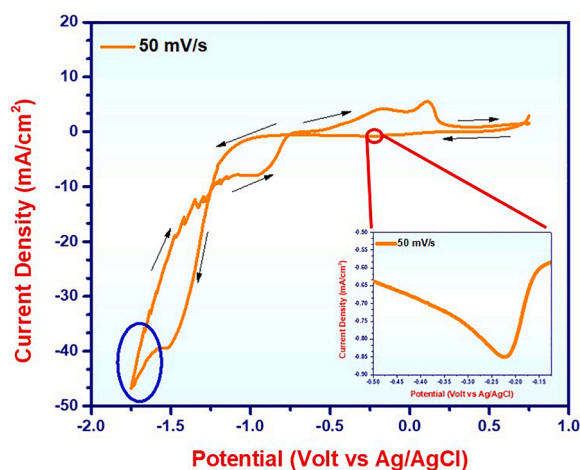


Fig. 1. Cyclic voltammetry (CV) study of HEA electrolyte containing sodium citrate and boric acid at pH ~ 2.5 at a scan rate of 50 mV/s. The inset image reveals the reduction peak corresponding to Cu. Blue circle indicates H_2 evolution beyond ~ -1.6 V.

microstructure/surface coverage of the thin films deposited with varied duty cycles is shown in Fig. 3, and it can be inferred that the surface coverage on the Ti increases as the duty cycle increases. For the LD sample, which has a duty cycle of 16.67% (duty cycle formula mentioned in Section 2.2), the surface coverage is observed to be the least as the effective deposition time is significantly low owing to the T_{on} (actual deposition time) which is small compared to the total pulse time ($T_{on} + T_{off}$). This surface coverage goes on increasing as the duty cycle reaches a maximum of 100%, i.e. on the DC sample. Similarly, for a fixed T_{on} with increasing T_{off} , (Fig. S2) the surface coverage also reduces as the duty cycle reduces with increasing T_{off} . Pulsed voltages containing alternative T_{on} and T_{off} were used where nucleation and growth can happen during the T_{on} pulse. During the T_{off} , reduction of metal ions from the electrolyte is stopped leading to a complete halt of the deposition process. As alternative cycles of T_{on} and T_{off} were used, a cyclic nature is established, where, during the next T_{on} , new nucleation centers are formed which can maximize the surface coverage. In addition, during T_{off} , the concentration of the ions near the cathode surface is replenished from the bulk leading to smoother depositions. DC electrodeposition may lead to the formation of dendritic growth owing to the continuous reduction of metal ions. However, to avoid the formation of dendritic growth we can use higher currents/voltages (limiting current) in PC, which leads to the incorporation of ions with higher reduction potentials into the growing film, i.e., a smooth, homogenous, and compact film can be obtained. In addition, the T_{off} also gives hydrogen bubbles sufficient time to escape without being incorporated into the electrodeposited film and helps in crack mitigation [25].

Not only the morphology/surface coverage of the electrodeposited thin films, but the composition of the electrodeposited thin films is also highly dependent on the duty cycles. This is especially in the case of alloys where multiple elements are simultaneously reduced during the electrodeposition process. To confirm the composition of the existing elements and their homogeneity in the electrodeposited thin films, EDS analysis was undertaken, and the data was acquired from a minimum of 9 equidistant areas throughout the sample (Fig. S3). The compositions in these five-element FeCoNiCuZn electrodeposits are majorly influenced by the T_{on} and T_{off} which in turn related to changes in the duty cycle that is determined by the formula $T_{on}(T_{on} + T_{off})^{-1}$. As seen in Fig. 4, with the increase in the duty cycle from LD to DC, the compositional change occurs majorly in the case of Cu. Higher T_{off} (lower duty cycles) seems to favor the formation of thin films in which Cu is seen to be greater than 50 at. % (Table S2). A similar effect was also observed during pulsed electrodeposition of Ni-Re and Ni-Cu alloys, where the composition of noble elements was higher at lower duty cycles [22,27,28].

For getting lower duty cycles, two possibilities exist, a) the T_{on} time must be as low as possible, and b) the T_{off} time must be as high as possible. If we consider the first possibility, i.e., the T_{on} is very low, then we have a scenario where before the start of the electroplating all the ions are present in their respective concentrations near the electrode. When the T_{on} starts, since Cu has a very high positive reduction potential, it has a higher tendency to get itself reduced in comparison to that of Cu. Additionally, Cu is reduced without the formation of any intermediates, whereas the others are reduced from the formation of adsorbed species which delays their reduction compared to Cu. Thus reduction of Cu is favoured, and hence the composition of the electrodeposited species is mostly Cu-rich in nature when the T_{on} is low and thus a large T_{on} effectively ensures a multi-element deposition. The SEM-EDS mapping of the HD and DC samples was also undertaken (Fig. S4), which revealed a homogenous distribution of all five elements.

The variation in the composition of all the individual elements at various T_{on} and T_{off} is plotted as contour diagrams (Fig. 5) which reveal an interesting trend. Higher T_{on} time favours the deposition of elements with negative reduction potentials (more anodic), and therefore, the percentages of Fe, Co, Ni, and Zn increase with increasing T_{on} . The

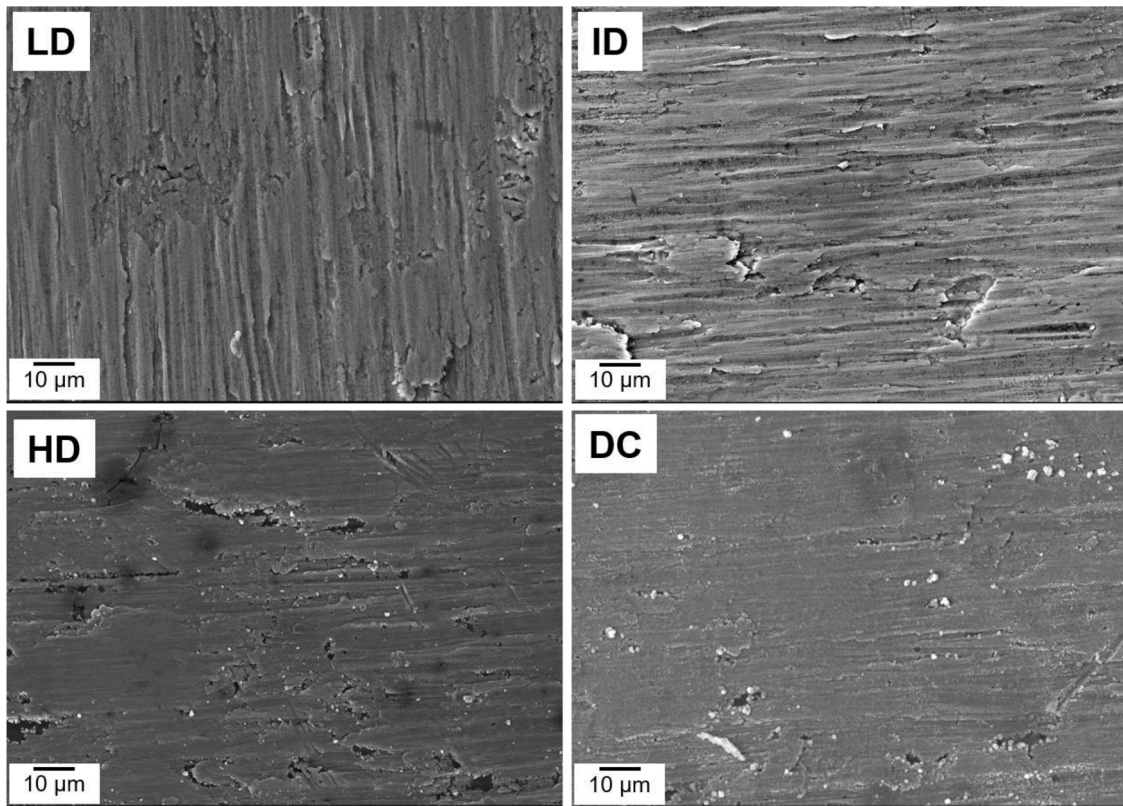


Fig. 2. Low magnification FE-SEM images of the LD, ID, HD, and DC samples deposited at various duty cycles.

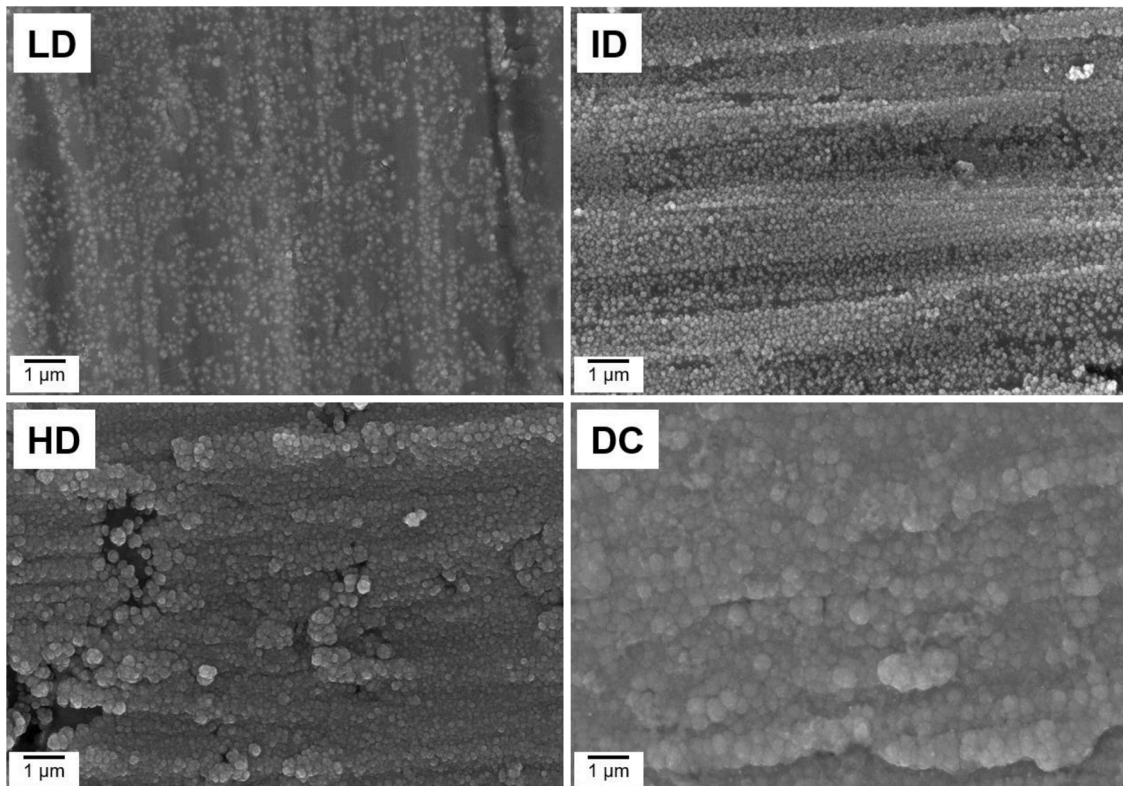


Fig. 3. High magnification FE-SEM images of the LD, ID, HD, and DC samples deposited at various duty cycles.

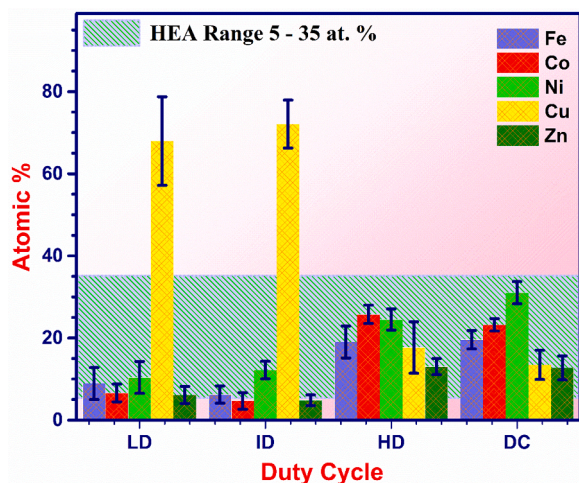


Fig. 4. SEM-EDS composition (at. %) of the LD, ID, HD, and DC samples.

tendency of these elements to reduce electrochemically may be influenced by the local pH, the presence of complexing agents, and their multiple stages of reduction, which can be majorly controlled by the applied T_{on} and T_{off} [17,29]. During electrodeposition, when the potential is applied, the metal ions that are present as per their respective concentrations in their oxidation states/complex form are sufficiently capable to get reduced to their metallic form. However, depending on their nature/ability (cathodic or anodic) among the five elements, the reduction of Cu is more favoured on account of two reasons, 1) thermodynamically, Cu is the noblest (electrochemically) among the available five elements for reduction 2) Cu reduction does not proceed via intermediates, unlike Fe, Co, Ni, and Zn which progress via intermediate adsorption. Thus, higher T_{on} gives Fe, Co, Ni and Zn enough time to get reduced leading to their incorporation in the electrodeposited thin film. In other words, higher T_{on} leads to larger incorporation of other elements which enables the ions that are reduced in multi-steps at the electrode-electrolyte interface to be incorporated in the electrodeposited thin film leading to a FeCoNiCuZn deposition [29]. For instance, $T_{on} > 10$ ms leads to multi-element deposition and slowly goes from dominant copper to an almost equiatomic electrodeposition (HEA) as the T_{on} reaches 50 ms. The increase in the Cu concentrations observed in the present study can also be explained using Eq. (1) which has already been used for Ni-Cu related alloys [26,28,30,31].

$$\tau_{Cu} = \frac{K_b t_{Cu}}{T_{on}^2 f^2} \quad (1)$$

where τ_{Cu} is the Cu content in the electrodeposited thin film, t_{Cu} is the transition time in seconds, K_b is a constant for a given bath, T_{on} is the pulse ON time, and f is the frequency of the pulse. As seen from Eq. (1), the Cu content in the thin film reduces when T_{on} increases or if the frequency is high. Similar results are also being observed in the present work, where with increasing T_{on} , lower Cu content is seen (Fig. 6) in the electrodeposited thin films, and the electrodeposition of other elements is also favoured. In addition, along with the T_{on} , T_{off} also plays an important role in controlling the composition for a given duty cycle. For a given T_{on} , as the T_{off} time increases, the Cu concentration is seen to increase. This is owing to the deposition of Cu during T_{off} where galvanic displacement reactions (GDR) also come into effect, which can increase the Cu content as the elements with extreme positive (Cu) and negative reduction (Fe, Co, Ni, and Zn) potentials can form a galvanic couple during the T_{off} [32]. However, the applied T_{off} in the current study has been optimized such that the $T_{off} < T_{on}$ to ensure the availability of metal ions at the electrode surface and to minimize the galvanic displacement reactions [33,34].

To understand the effect of duty cycles on the roughness of the

electrodeposited thin films, AFM studies (Fig. S5) were also undertaken. The roughness of the electrodeposited FeCoNiCuZn film is lower at lower duty cycles. However, the lower surface coverage (very low effective deposition time) for a given deposition time leads to a standard deviation of 29 nm. The root mean square (RMS) roughness for the LD samples stood at 72 ± 29 nm, and it was noted that the roughness of the films increases as the duty cycle (T_{on}) increases. The T_{off} plays an important role in aiding surface diffusion to allow smooth film formation, ion replenishment to happen in the diffusion layer, and overall helps to prevent dendritic growth thereby improving the smoothness of the thin film. During higher duty cycles, T_{off} is reduced drastically such that these phenomena cannot take place sufficiently to ensure a smooth film formation, and hence the roughness increases. Therefore, the surface roughness of the DC sample (100 % duty cycle), which has no T_{off} is the highest at 151 ± 50 nm with very high standard deviation as expected.

After confirming the composition and morphology of the thin films as a function of the duty cycle, the crystal structure (Fig. 7a & Fig. 7b) analysis of the as-deposited thin films was undertaken by XRD, and the various cell/lattice parameters as determined by XRD are given in Table 1. Usually, the crystal structure of the electrodeposited alloy is dependent on the composition of the thin films, as already reported on similar systems like FeCoNi. In the FeCoNi system, for instance, a higher percentage of Fe in the alloy exhibits a BCC structure, whereas a higher percentage of Ni leads to an FCC structure [35–37]. Additionally, when Fe content in the films is low, the electrodeposited film is dominated by FCC Co and FCC Ni phases, and the phases are highly dependent on the composition of the electrodeposited thin films [38]. Since the current deposition has five elements with almost equal proportions of all the elements, predicting a crystal structure is more complex. To add to it, complex heterogeneities that occur in HEAs/MCAs [39] and the obvious random local galvanic displacement reactions during the T_{off} may influence a change in the local composition thereby changing the phase of the resulting thin film being electrodeposited. In the present work, the composition of the electrodeposited thin films is highly dependent on the duty cycles. For lower duty cycles, i.e. the LD and ID samples, higher percentage of Cu is present in the thin film, whereas in HD and DC, multi-element deposition in range of 5 – 35 at.% (HEA) is observed. Therefore, the XRD patterns for both the LD and ID gave rise to a peak centered at a 2θ of $\sim 43.30^\circ$ corresponding closely to that of metallic Cu owing to the higher at.% of Cu in the deposited films. On the contrary, the HD and DC samples on account of multiple elements (HEA) including Fe, Co, and Ni showed a peak shift from the LD and ID samples towards higher 2θ values indicating the HEA formation. More precisely, the electrodeposited HD sample gave rise to an FCC phase with a 2θ centered at 43.56° for a given deposition time of 5 min with a duty cycle of 83.33%. The electrodeposited DC sample which has higher percentage of Ni (in comparison to HD) led to a peak shift towards higher 2θ values and gave rise to an FCC phase with the peak centered at a 2θ of 43.72° for a given deposition time of 5 min having 100% duty cycle. However, as the deposition time/thickness of the deposited film increases a dual BCC + FCC phase for the same alloy has also been reported [17], and powders of the same alloy system prepared by ball milling have indicated a single FCC phase [40,41].

3.3. Substrate roughness and pH

From the study of the morphology and composition using FE-SEM and EDS, it can be concluded that LD and ID did not yield homogeneous distribution of the intended elements, whereas DC, despite multi-element deposition, shows higher surface roughness. Thus, the HD condition is the best suited for HEA thin film deposition, and this condition was chosen to study the effect of substrate roughness and pH on the composition and morphology of the electrodeposited samples. Surface roughness is a unique parameter that can affect compositions dur-

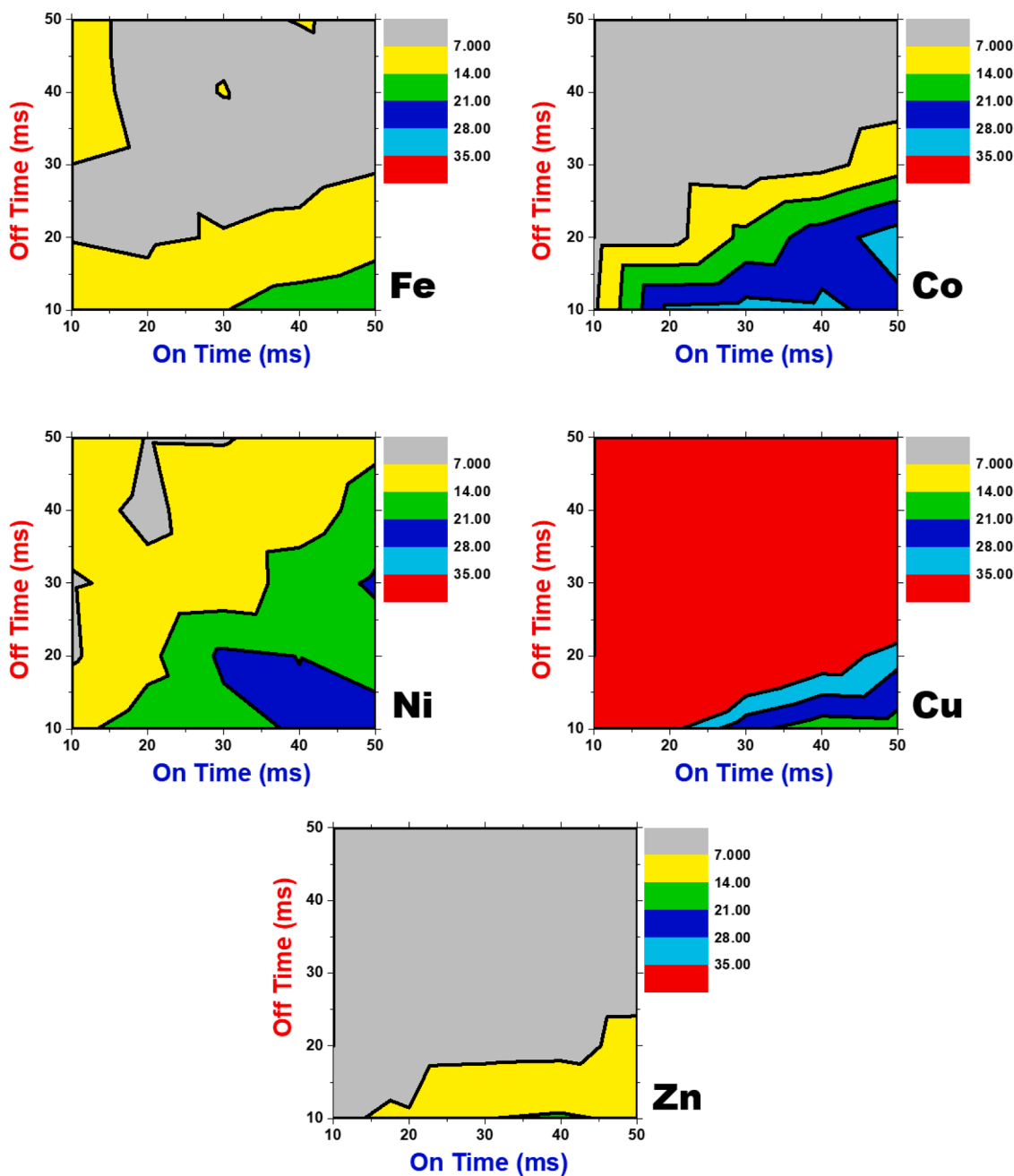


Fig. 5. Contour maps of the composition of different elements deposited at various T_{on} & T_{off} .

ing the electrodeposition of multi-elemental systems consisting of different elements owing to the changes in the diffusion layer thickness, which results from the roughness of the electrode [21]. Additionally, the induced roughness creates crests where the current density is higher and troughs where the current density is lower, leading to differential compositions of the electrodeposited thin film at these local spots. Further, the local pH at the electrode-electrolyte interface influences the concentration of OH^- ions that can react with the metal ions at the interface and often form non-soluble oxides/hydroxides, which can hinder the reduction of other elements during the electrodeposition. Therefore, to understand the role of the surface roughness of the substrate and the pH of the electrolyte on the composition of the FeCoNiCuZn thin film, several experiments at the HD condition were undertaken where Ti substrates (Figs. S6, S7) of different levels of roughness were used and the composition of the electrodeposited thin films was evaluated from the EDS analysis. Simultaneously, the role of

pH with respect to the surface roughness of the substrate was also studied. The role of substrate roughness and the pH of the electrolyte in controlling the composition of the FeCoNiCuZn thin film have been plotted as contour maps, shown in Fig. 8. From the contour maps, it can be concluded that the surface roughness does not affect the composition of the electrodeposited thin film. This is on account of the HD condition comprising of pulses which may probably aid in ensuring a homogenous composition owing to the uniformity in reduction/nucleation of all the elements simultaneously during the applied pulses. However, unlike the substrate roughness, pH has been shown to have a significant effect in varying the composition of the electrodeposited FeCoNiCuZn thin films, which can be observed from the contour map in Fig. 8.

Though the application of pulses may aid in achieving uniform composition with homogenous distribution, the pH of the electrolyte plays a significant role at the electrode-electrolyte interface during the deposition. It is well known that electrodeposition in an aqueous

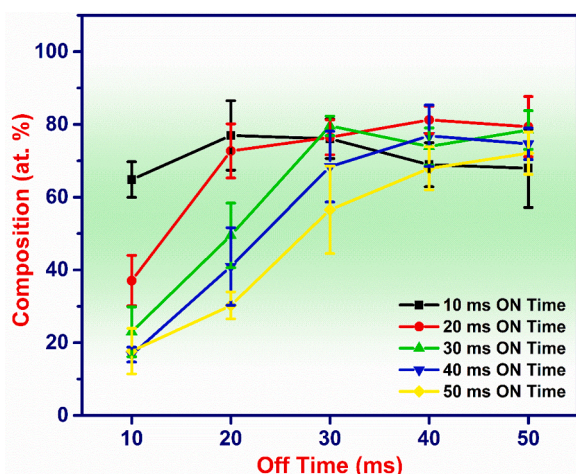


Fig. 6. Copper composition in the various electrodeposited FeCoNiCuZn thin films at different T_{on} & T_{off} .

medium has a challenge of H_2 evolution, especially in the case of alloy deposition, and deposition composition varies predominantly depending on the local pH at the electrode-electrolyte interface, which is often different from the bulk pH. Therefore, depositions at pH from 0.5 to 4.5 were performed to understand the deposition behavior of each element during the reduction at the cathode. At pH = 0.5, as the electrolyte is highly acidic, vigorous H_2 evolution was taking place, and the entire available active substrate area was covered with bubbles that hindered deposition. This may probably be because of the reduction of H^+ ions which is favored thermodynamically since its reduction potential is higher than that of the metal ions present in the electrolyte. In addition, the reduced H^+ ions escaped as H_2 bubbles that caused non-uniform reduction where metallic deposition is virtually non-existent. As the pH increases from 0.5 to 4.5, the hydrogen evolution seems to decrease, thereby resulting in improved quality of the deposition. However, an acidic pH of 1.5 leads to a Cu favoured deposition (Cu reduction favoured at acidic pH) where the deposited film has a copper tinge. Further increasing the pH towards 2.5, 3.5, and 4.5 leads to a change in the deposited thin film color from copper tinge to a metallic coating with a silvery grey finish which confirms the simultaneous reduction of Fe, Co, Ni, Cu, and Zn resulting in HEA composition. The FE-SEM images are seen in Fig. 9 where, at a low pH, i.e., pH (0.5 & 1.5), irregularly deposited film with spherical islands was observed. Only films deposited at pH = 2.5 showed complete uniform coverage. Even though

depositions at pH = 3.5 showed uniform coverage, they were found to have cracks. These cracks gradually increased in size when the pH was 4.5. The composition analyses by EDS (Fig. 10) reveal that Cu is majorly deposited at pH = 0.5 & 1.5. Near equal composition of all the elements is seen at pH = 2.5 (crack-free), 3.5 & 4.5. The electrodeposition of the metal ions used in the present study is always accompanied by the production of H_2 gas at the cathode owing to the aqueous medium used. Hydroxides can be readily available at a higher pH, often resulting in hydroxide formation of the electrode and this can lead to crack formation. This can be addressed by the use of boric acid which aids in allaying these rapid changes in pH near the cathode that can minimize the crack formation [42]. From the experimental observations, even though the pH from 2.5 to 4.5 did not lead to major compositional changes in the thin film, the film quality is seen to be compromised (Fig. 9), and prominent cracks can be noticed. The formation of cracks as the pH changes from pH 2.5 to 4.5 could be arising from the presence of the OH^- ions leading to the precipitation at the electrode-electrolyte interface during the deposition, which causes major cracks on the electrodeposit. Additionally, if the pH of the electrolyte ≥ 5 , it leads to the precipitation of the metal salts making the electrolyte unstable and opaque, and hence depositions beyond pH = 4.5 could not be possible at all. Therefore, the optimum pH of the electrolyte has to be maintained by considering the stability of the ions in the electrolyte.

The compositional variations at pH from 0.5 to 4.5 in the electrodeposited thin films can be understood from the behavior/activity of individual metal ions and their stability during the deposition at the electrode. In addition, along with the pH, the electrodeposition of the individual element is also majorly dependent on the presence of other elements as well. Fe group elements in the present case FeCoNiCuZn usually undergo anomalous deposition, which often changes the kinetics of the deposition and can lead to significant composition variation. Better understanding and correlating the behavior of each element in the alloy can be considered by using the composition ratio value (CRV). The CRV (Eq. (2)) can be calculated using the formula proposed by Yang et al. [43]

Table 1
Unit Cell parameters as determined by XRD.

Sample	2 θ (degree)	d spacing (nm)	a (nm)
LD	43.32	0.2086	0.3613
ID	43.30	0.2087	0.3615
HD	43.56	0.2075	0.3594
DC	43.72	0.2068	0.3582

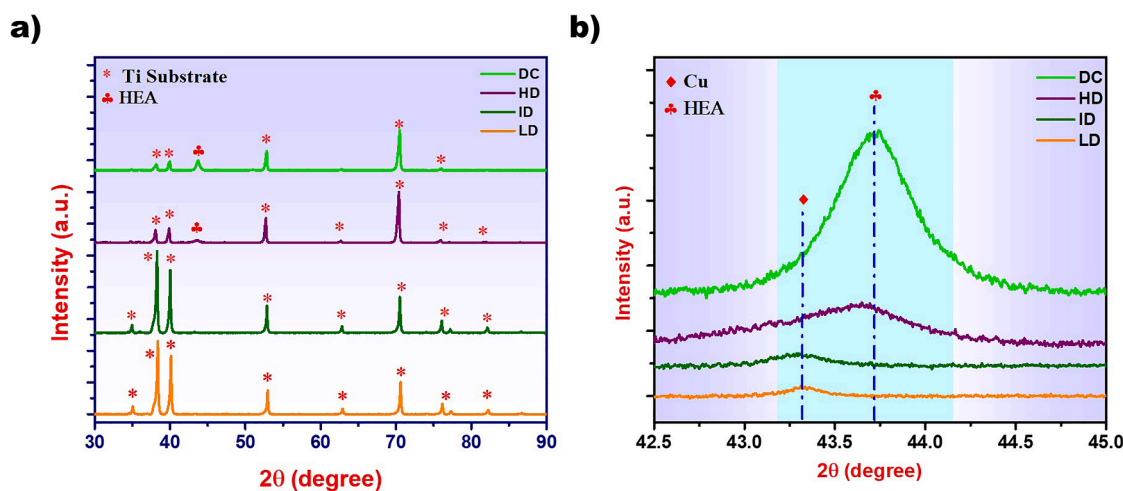


Fig. 7. (a) XRD patterns of the samples synthesized at various duty cycles, i.e., LD, ID, HD, and DC. (b) Zoomed XRD patterns of the various samples from 42.5° to 45.0° degrees.

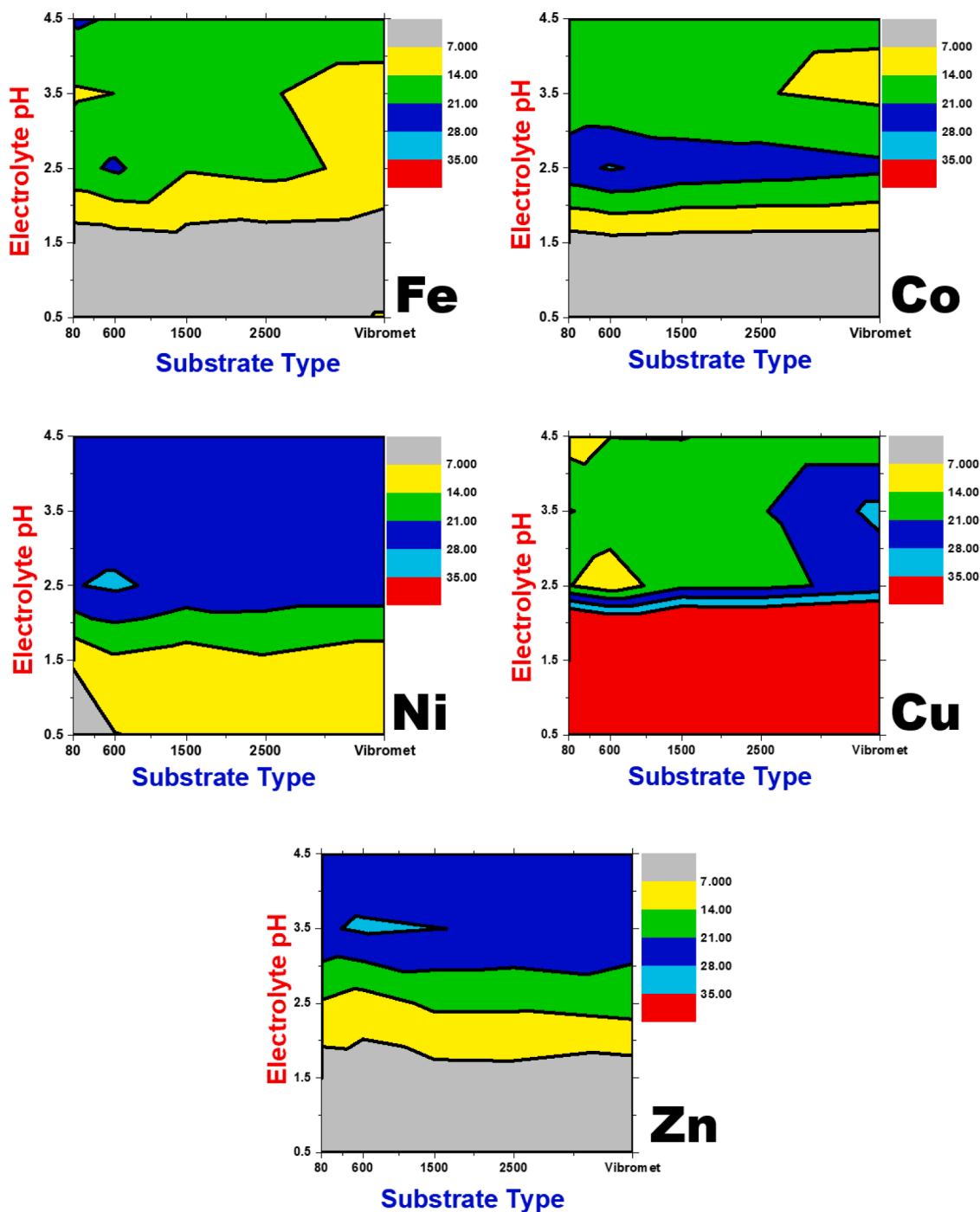


Fig. 8. Contour plots of the compositions of various elements in the electrodeposited samples at various electrolyte pH and substrate types (surface roughness).

$$CRV = \frac{\text{wt.\% of element in electrodeposited alloy}}{\text{wt.\% of element in electrolyte}} \quad (2)$$

According to Yang et al., if $CRV < 1$, then the element can be considered to be deposited normally, whereas if $CRV > 1$, then the element is considered to be deposited anomalously. However, as the number of elements increases, the deposition kinetics may vary significantly, and in the current scenario of FeCoNiCuZn, the electrolyte composition was optimized in such a way as to achieve the required composition of each element in the alloy to minimize the anomalous deposition. Electrodeposition of binary alloys of the Fe group elements shows anomalous deposition, and these elements together also show anomalous deposition in the presence of other metal ions, in the current

case, Zn [44]. Thus, based on the CRV values, the individual element behavior during the electrodeposition with respect to the electrolyte pH can give us more understanding of the sensitivity of each element in the presence of other elements during the simultaneous reduction. A table containing the CRV values of the elements in the current deposited thin films at various pH is given in Table 2, where it is observed that at low pH, the CRV value for Cu is very high ~ 30 (at $pH \leq 1.5$) and reduces drastically to ~ 8 (at $pH \geq 2.5$) which are in the regime of anomalous deposition. This anomalous behavior of Cu is due to the cathodic nature of Cu at acidic pH. Similarly, more anodic Zn has a CRV value of < 1 at $pH = 0.5$ & $pH = 1.5$ and enters into the anomalous regime at $pH \geq 2.5$, probably owing to the precipitation and formation of Zn hydroxides that have a lower solubility [45]. This precipitation eventually inhibits the

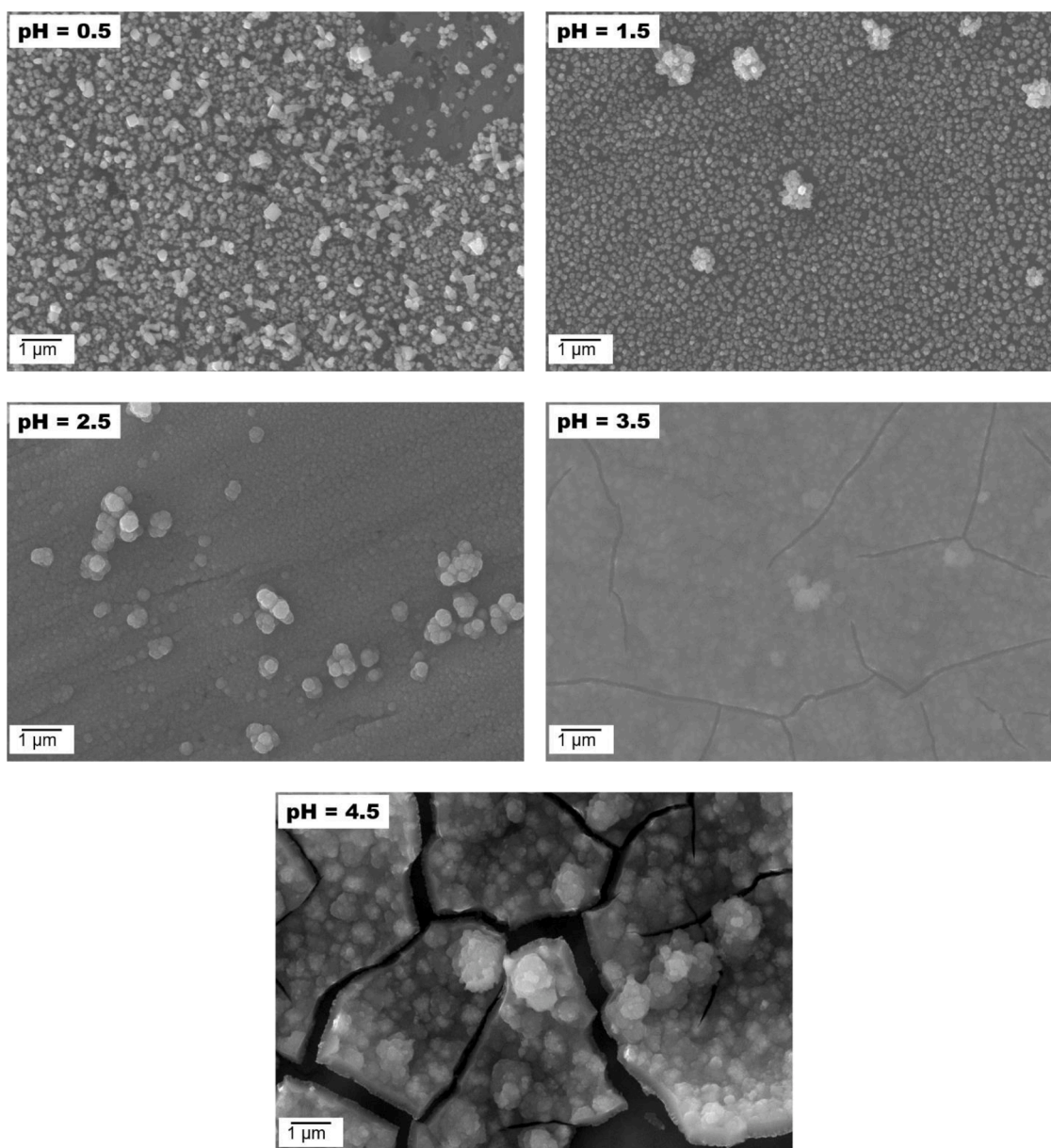


Fig. 9. FE-SEM images of the electrodeposited samples on a 2500 grit polished Ti substrate using HD conditions at various pH.

reduction of other metal ions by covering the entire surface of the cathode and results in increasing Zn content in the electrodeposited FeCoNiCuZn thin film. To reduce this anomalous deposition of both Cu and Zn, their concentration in the electrolyte is reduced to a bare minimum, as mentioned in the experimental section. At the outset, complex diffusion mechanisms, surface kinetics, and concentration of the metal species play a major role in ensuring near equiatomic multi-element deposition, especially in achieving the required composition in the HEA range.

4. Conclusion

The role of various experimental parameters, such as duty cycles (varying T_{on} & T_{off}), the surface roughness of the substrate, and electrolyte pH have been studied in controlling the composition of FeCoNiCuZn thin films. From the observations, duty cycle, and pH were found to play a significant role in controlling the microstructure and composition of the FeCoNiCuZn thin films. Whereas, due to the application of pulses during the electrodeposition, the surface roughness of

the substrate was found to have a negligible effect on the microstructure and composition. From the study, it can also be interpreted that for the electrodeposition of multiple elements, the T_{on} time must be higher than the T_{off} for simultaneous deposition of multiple elements as alloys, especially in the case of elements with extreme reduction potentials. Higher T_{on} with higher duty cycles (> 0.75) leads to the electrodeposition of multi-elemental (FeCoNiCuZn) thin film systems with the required HEA composition. On the other hand, electrolyte pH ($= 0.5$ & 1.5) leads to a favoured deposition of Cu, and as pH increases to pH = 2.5 , FeCoNiCuZn HEA deposition with better film quality can be attained. At higher pH (≥ 3.5), crack formation is visible, which may compromise the structural integrity of the electrodeposited thin films. Hence, electrolyte composition with controlled duty cycles and optimum pH can result in crystalline HEA thin films with the required composition. Finally, this study provides more insights into the understanding of the simultaneous deposition of multi-element (≥ 5) depositions in an aqueous medium which can be explored for numerous multi-metallic alloy systems.

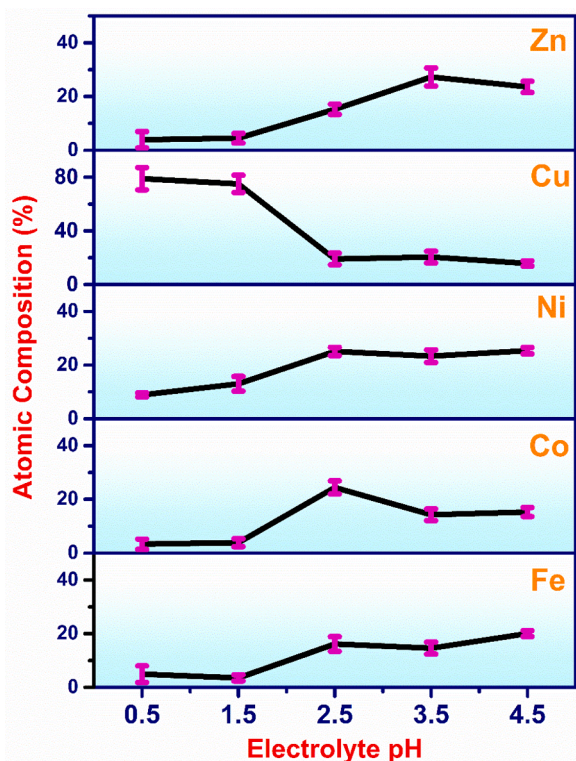


Fig. 10. The composition of the different elements in the electrodeposited thin films at different pH.

Table 2

Composition ratio values (CRV) of various elements in the electrodeposited samples under HD conditions at different pH.

pH	Fe	Co	Ni	Cu	Zn
0.5	0.187	0.126	0.197	29.898	0.603
1.5	0.134	0.147	0.290	28.473	0.692
2.5	0.637	0.966	0.579	7.514	2.417
3.5	0.568	0.556	0.531	7.953	4.267
4.5	0.788	0.602	0.583	6.153	3.727

CRedit authorship contribution statement

Kunda Siri Kiran Janardhana Reddy: Methodology, Validation, Formal analysis, Investigation, Writing – original draft, Data curation, Visualization. **L.P. Pavithra Chokkakula:** Conceptualization, Methodology, Validation, Formal analysis, Investigation, Writing – review & editing, Visualization. **Suhash Ranjan Dey:** Conceptualization, Resources, Writing – review & editing, Supervision, Project administration, Funding acquisition.

Declaration of Competing Interest

The authors declare that they have no known competing financial interests or personal relationships that could have appeared to influence the work reported in this paper. Chokkakula L.P. Pavithra, Reddy Kunda Siri Kiran Janardhana and Suhash Ranjan Dey has patent #Electrochemical synthesis of nanocrystalline multicomponent alloy thin films/coatings in an aqueous medium (Indian Patent, Application No. 201941013178) pending to Indian Institute of Technology Hyderabad.

Acknowledgments

The authors acknowledge the research facilities at the Department of Materials Science & Metallurgical Engineering, IIT Hyderabad, for

facilitating the characterization of this work.

Supplementary materials

Supplementary material associated with this article can be found, in the online version, at doi:10.1016/j.electacta.2023.142350.

References

- [1] J.W. Yeh, S.K. Chen, S.J. Lin, J.Y. Gan, T.S. Chin, T.T. Shun, C.H. Tsau, S.Y. Chang, Nanostructured high-entropy alloys with multiple principal elements: novel alloy design concepts and outcomes, *Adv. Eng. Mater.* 6 (2004) 299–303, <https://doi.org/10.1002/adem.200300567>.
- [2] S. Ranganathan, Alloyed pleasures: multimetallic cocktails, *Curr. Sci.* 85 (2003) 1404–1406.
- [3] S.K. Padamata, A. Yasinskiy, V. Yanov, G. Saevarsdottir, Magnetron sputtering high-entropy alloy coatings: a mini-review, *Metals* 12 (2022) 319, <https://doi.org/10.3390/met12020319>. Basel.
- [4] M.D. Cropper, Thin films of AlCrFeCoNiCu high-entropy alloy by pulsed laser deposition, *Appl. Surf. Sci.* 455 (2018) 153–159, <https://doi.org/10.1016/j.apsusc.2018.05.172>.
- [5] T.W. Lu, C.S. Feng, Z. Wang, K.W. Liao, Z.Y. Liu, Y.Z. Xie, J.G. Hu, W.B. Liao, Microstructures and mechanical properties of CoCrFeNiAl_{0.3} high-entropy alloy thin films by pulsed laser deposition, *Appl. Surf. Sci.* 494 (2019) 72–79, <https://doi.org/10.1016/j.apsusc.2019.07.186>.
- [6] C.Z. Yao, P. Zhang, M. Liu, G.R. Li, J.Q. Ye, P. Liu, Y.X. Tong, Electrochemical preparation and magnetic study of Bi-Fe-Co-Ni-Mn high entropy alloy, *Electrochim. Acta* 53 (2008) 8359–8365, <https://doi.org/10.1016/j.electacta.2008.06.036>.
- [7] C. Yao, B. Wei, P. Zhang, X. Lu, P. Liu, Y. Tong, Facile preparation and magnetic study of amorphous Tm-Fe-Co-Ni-Mn multicomponent alloy nanofilm, *J. Rare Earths* 29 (2011) 133–137, [https://doi.org/10.1016/S1002-0721\(10\)60418-8](https://doi.org/10.1016/S1002-0721(10)60418-8).
- [8] Q. Li, Z. Feng, J. Zhang, P. Yang, F. Li, M. An, Pulse reverse electrodeposition and characterization of nanocrystalline zinc coatings, *RSC Adv.* 4 (2014) 52562–52570, <https://doi.org/10.1039/c4ra09421b>.
- [9] V. Soare, M. Burada, I. Constantin, D. Mitrice, V. Bødilite, A. Caragea, M. Tärcolea, Electrochemical deposition and microstructural characterization of AlCrFeMnNi and AlCrCuFeMnNi high entropy alloy thin films, *Appl. Surf. Sci.* 358 (2015) 533–539, <https://doi.org/10.1016/j.apsusc.2015.07.142>.
- [10] J. Sure, D.S.M. Vishnu, C. Schwandt, Direct electrochemical synthesis of high-entropy alloys from metal oxides, *Appl. Mater. Today* 9 (2017) 111–121, <https://doi.org/10.1016/j.apmt.2017.05.009>.
- [11] J. Sure, D. Sri Maha Vishnu, C. Schwandt, Electrochemical conversion of oxide spinels into high-entropy alloy, *J. Alloys Compd.* 776 (2019) 133–141, <https://doi.org/10.1016/j.jallcom.2018.10.171>.
- [12] J. Sure, D. Sri Maha Vishnu, C. Schwandt, Preparation of refractory high-entropy alloys by electro-deoxidation and the effect of heat treatment on microstructure and hardness, *JOM* 72 (2020) 3895–3905, <https://doi.org/10.1007/s11837-020-04367-2>.
- [13] W. Simka, D. Puszczczyk, G. Nawrat, Electrodeposition of metals from non-aqueous solutions, *Electrochim. Acta* 54 (2009) 5307–5319, <https://doi.org/10.1016/j.electacta.2009.04.028>.
- [14] A. Aliyu, C. Srivastava, Microstructure and corrosion properties of MnCrFeCoNi high entropy alloy-graphene oxide composite coatings, *Materialia* 5 (2019), 100249, <https://doi.org/10.1016/j.mta.2019.100249>.
- [15] M. Dehestani, S. Sharafi, G.R. Khayati, The effect of pulse current density on the microstructure, magnetic, mechanical, and corrosion properties of high-entropy alloy coating Fe-Co-Ni-Mo-W, achieved through electro co-deposition, *Intermetallics* 147 (2022), 107610, <https://doi.org/10.1016/j.intermet.2022.107610>.
- [16] D. Ahmadkhanika, J. Kruemling, C. Zanella, Electrodeposition of high entropy alloy of Ni-Co-Cu-Mo-W from an aqueous bath, *J. Electrochem. Soc.* 169 (2022), 082515, <https://doi.org/10.1149/1945-7111/ac87d5>.
- [17] C.L.P. Pavithra, R.K.S.K. Janardhana, K.M. Reddy, C. Murapaka, J. Joardar, B.V.S. arada, R.R. Tamboli, Y. Hu, Y. Zhang, X. Wang, S.R. Dey, An advancement in the synthesis of unique soft magnetic CoCuFeNiZn high entropy alloy thin films, *Sci. Rep.* 11 (2021) 8836, <https://doi.org/10.1038/s41598-021-87786-8>.
- [18] C.L.P. Pavithra, R.K. Siri Kiran Janardhana, K. Madhav Reddy, C. Murapaka, X. Wang, S.R. Dey, One-dimensional Co-Cu-Fe-Ni-Zn high-entropy alloy nanostructures, *Mater. Res. Lett.* 9 (2021) 285–290, <https://doi.org/10.1080/21663831.2021.1896588>.
- [19] F. Yoosefan, A. Ashrafi, S.M. Monir vaghefi, I. Constantin, Synthesis of CoCrFeMnNi high entropy alloy thin films by pulse electrodeposition: part 1: effect of pulse electrodeposition parameters, *Met. Mater. Int.* 26 (2020) 1262–1269, <https://doi.org/10.1007/s12540-019-00404-1>.
- [20] F. Yoosefan, A. Ashrafi, S.M. Monir vaghefi, Characterization of Co-Cr-Fe-Mn-Ni high-entropy alloy thin films synthesized by pulse electrodeposition: part 2: effect of pulse electrodeposition parameters on the wettability and corrosion resistance, *Met. Mater. Int.* 27 (2021) 106–117, <https://doi.org/10.1007/s12540-019-00584-w>.
- [21] S.H. Jeon, W.I. Choi, G.D. Song, Y.H. Son, D. Hur, Influence of surface roughness and agitation on the morphology of magnetite films electrodeposited on carbon steel substrates, *Coatings* 6 (2016) 62, <https://doi.org/10.3390/coatings6040062>.

- [22] D. Landolt, A. Marlot, Microstructure and composition of pulse-plated metals and alloys, *Surf. Coat. Technol.* 169–170 (2003) 8–13, [https://doi.org/10.1016/S0257-8972\(03\)00042-2](https://doi.org/10.1016/S0257-8972(03)00042-2).
- [23] A. Mallik, B.C. Ray, Evolution of principle and practice of electrodeposited thin film: a review on effect of temperature and sonication, *Int. J. Electrochem.* 2011 (2011) 1–16, <https://doi.org/10.4061/2011/568023>.
- [24] A. Dolati, M. Sababi, E. Nouri, M. Ghorbani, A study on the kinetic of the electrodeposited Co-Ni alloy thin films in sulfate solution, *Mater. Chem. Phys.* 102 (2007) 118–124, <https://doi.org/10.1016/j.matchemphys.2006.07.009>.
- [25] Y. Deo, R. Ghosh, A. Nag, D.V. Kumar, R. Mondal, A. Banerjee, Direct and pulsed current electrodeposition of Zn-Mn coatings from additive-free chloride electrolytes for improved corrosion resistance, *Electrochim. Acta* 399 (2021), 139379, <https://doi.org/10.1016/j.electacta.2021.139379>.
- [26] S.K. Ghosh, A.K. Grover, G.K. Dey, M.K. Totlani, Nanocrystalline Ni-Cu alloy plating by pulse electrolysis, *Surf. Coatings Technol.* 126 (2000) 48–63, [https://doi.org/10.1016/S0257-8972\(00\)00520-X](https://doi.org/10.1016/S0257-8972(00)00520-X).
- [27] T. Nusbaum, B.A. Rosen, E. Gileadi, N. Eliaz, Effect of pulse on-time and peak current density on pulse plated Re-Ni alloys, *J. Electrochem. Soc.* 162 (2015) D250–D255, <https://doi.org/10.1149/2.0111507jes>.
- [28] M. Cherkaoui, E. Chassaing, K. Vu Quang, Pulse plating of Ni-Cu alloys, *Surf. Coat. Technol.* 34 (1988) 243–252, [https://doi.org/10.1016/0257-8972\(88\)90116-8](https://doi.org/10.1016/0257-8972(88)90116-8).
- [29] Qiang Huang, Electrodeposition of FeCoNiCu quaternary system (2004). LSU Doctoral Dissertations. 732. https://digitalcommons.lsu.edu/gradschool_dissertations/732.
- [30] S. Roy, An analytical equation to compute the composition of pulse-plated binary alloys, *Plat. Surf. Finish.* 86 (1999) 76–79.
- [31] P.E. Bradley, B. Janossy, D. Landolt, Pulse plating of cobalt-iron-copper alloys, *J. Appl. Electrochem.* 31 (2001) 137–144, <https://doi.org/10.1023/A:1004155000693>.
- [32] A. Papaderakis, I. Mintsouli, J. Georgieva, S. Sotiropoulos, Electrocatalysts prepared by galvanic replacement, *Catalysts* 7 (2017) 80, <https://doi.org/10.3390/catal7030080>.
- [33] S. Roy, D. Landolt, Effect of off-time on the composition of pulse-plated Cu-Ni alloys, *J. Electrochem. Soc.* 142 (1995) 3021–3027, <https://doi.org/10.1149/1.2048679>.
- [34] S. Roy, M. Matlosz, D. Landolt, Effect of corrosion on the composition of pulse-plated Cu-Ni alloys, *J. Electrochem. Soc.* 141 (1994) 1509–1517, <https://doi.org/10.1149/1.2054954>.
- [35] X. Liu, G. Zangari, M. Shamsuzzoha, Structural and magnetic characterization of electrodeposited, high moment FeCoNi films, *J. Electrochem. Soc.* 150 (2003) C159, <https://doi.org/10.1149/1.1545462>.
- [36] D.Y. Park, B.Y. Yoo, S. Kelcher, N.V.M. Yung, Electrodeposition of low-stress high magnetic moment Fe-rich FeCoNi thin films, *Electrochim. Acta* 51 (2006) 2523–2530, <https://doi.org/10.1016/j.electacta.2005.07.037>.
- [37] B.Y. Yoo, S.C. Hernandez, D.Y. Park, N.V.M. Yung, Electrodeposition of FeCoNi thin films for magnetic-MEMS devices, *Electrochim. Acta* 51 (2006) 6346–6352, <https://doi.org/10.1016/j.electacta.2006.04.020>.
- [38] H. Kockar, O. Demirbas, H. Kuru, M. Alper, O. Karaagac, M. Haciismailoglu, E. Ozergin, Electrodeposited NiCoFe films from electrolytes with different Fe ion concentrations, *J. Magn. Magn. Mater.* 360 (2014) 148–151, <https://doi.org/10.1016/j.jmmm.2014.01.078>.
- [39] E. Ma, X. Wu, Tailoring heterogeneities in high-entropy alloys to promote strength–ductility synergy, *Nat. Commun.* 10 (2019) 5623, <https://doi.org/10.1038/s41467-019-13311-1>.
- [40] Z. Yingzhe, C. Yudaο, Q. Qingdong, L. Wei, Synthesis of FeCoNiCuZn single-phase high-entropy alloy by high-frequency electromagnetic-field assisted ball milling, *J. Magn. Magn. Mater.* 498 (2020), 166151, <https://doi.org/10.1016/j.jmmm.2019.166151>.
- [41] V.K. Soni, S. Sanyal, S.K. Sinha, Investigation of phase stability of novel equiatomic FeCoNiCuZn based-high entropy alloy prepared by mechanical alloying, *AIP Conf. Proc.* (2018) 1953, <https://doi.org/10.1063/1.5032588>.
- [42] R.C.M. Salles, G.C.G. De Oliveira, S.L. Díaz, O.E. Barcia, O.R. Mattos, Electrodeposition of Zn in acid sulphate solutions: PH effects, *Electrochim. Acta* 56 (2011) 7931–7939, <https://doi.org/10.1016/j.electacta.2010.12.026>.
- [43] Y. Yang, Preparation of Fe-Co-Ni ternary alloys with electrodeposition, *Int. J. Electrochem. Sci.* 10 (2015) 5164–5175.
- [44] Z. Zhou, T.J. O’Keefe, Modification of anomalous deposition of Zn-Ni alloy by using tin additions, *Surf. Coat. Technol.* 96 (1997) 191–197, [https://doi.org/10.1016/S0257-8972\(97\)00111-4](https://doi.org/10.1016/S0257-8972(97)00111-4).
- [45] A.C. Hegde, K. Venkatakrishna, N. Eliaz, Electrodeposition of Zn-Ni, Zn-Fe and Zn-Ni-Fe alloys, *Surf. Coat. Technol.* 205 (2010) 2031–2041, <https://doi.org/10.1016/j.surfcoat.2010.08.102>.